



# Experimental Study of the Ternary Phase Diagram Al–Ge–Mg

Ondřej Zobač<sup>1</sup> · Lenka Karpišková<sup>1,2</sup> · Aleš Kroupa<sup>1</sup>

Submitted: 12 September 2022 / in revised form: 24 November 2022 / Accepted: 21 December 2022 / Published online: 8 February 2023  
© ASM International 2023

**Abstract** The phase equilibria of the Al–Ge–Mg ternary phase diagram were experimentally studied at the temperatures of 250, 300, 400 and 450 °C. The ternary phase  $\tau$  ( $\text{Al}_2\text{Ge}_2\text{Mg}$ ) suggested by the earlier structural study was found to be stable at all temperatures studied. Detailed study of the phase equilibria containing the  $\tau$  ( $\text{Al}_2\text{Ge}_2\text{Mg}$ ) phase in the ternary system have been carried out. The average composition of this phase was found to be 36 at.% Al–36 at.% Ge–Mg. In contrast to the previously published binary Ge–Mg phase diagram, the solubility of Mg in Ge was found to be within a few atomic percent. It was also found that  $\text{GeMg}_2$  intermetallic phase dissolves only small amount of Al but there is significant nonstoichiometricity with respect to the Ge/Mg ratio especially for lower annealing temperatures.

**Keywords** Al–Ge–Mg phase diagram · SEM · ternary phase · XRD

## 1 Introduction and Literature Review

The Al–Mg binary system is widely used as a basis for lightweight structural materials. The use of Germanium as an alloying element should contribute to the improvement of the properties of this alloy at higher temperatures due to

its similarity of germanium with silicon which is commonly used.<sup>[1]</sup>

Knowledge of ternary phase equilibria in the entire concentration and temperature range is crucial for the design of new promising alloys. Unfortunately, works focused on this aspect of the Al–Ge–Mg system are quite few. Phase equilibria in the system were studied only in the works of Badaeva and Kuznetsova<sup>[2]</sup> and Legka et al.<sup>[3]</sup> Pukas<sup>[4]</sup> identified one  $\text{Al}_2\text{Ge}_2\text{Mg}$  ternary phase in this system and described its crystal structure, but did not present any results on its phase equilibria in the ternary system.

## 2 Al–Ge Binary System

The Al–Ge binary alloy is a basic eutectic system where the position of the eutectic point is approx. 72 at.% Al and 424 °C. The mutual solubility of both elements is relatively small. (see Fig. 1a). The binary system has been studied by several authors.<sup>[5–8]</sup> Figure 1(a) represent the experimental binary phase diagram of Al–Ge subsystem proposed by McAllister and Murray<sup>[7]</sup>

## 3 Al–Mg Binary System

The binary phase diagram of the Al–Mg system (see Fig. 1b) is very well described experimentally and theoretically in the literature e.g.<sup>[9–11]</sup> In this system, there are three stable intermetallic phases with non-negligible solubility. The  $\beta$ -AlMg phase is stable up to 450 °C,  $\gamma$ -AlMg melts congruently at 457 °C, and  $\varepsilon$ -AlMg exists in the temperature range 193–417 °C. The experimental binary

✉ Ondřej Zobač  
zobac@ipm.cz

<sup>1</sup> Institute of Physics of Materials, The Czech Academy of Sciences, Žitkova 22, 616 00 Brno, Czech Republic

<sup>2</sup> Faculty of Science, Masaryk University, Kotlarska 22, 616 00 Brno, Czech Republic

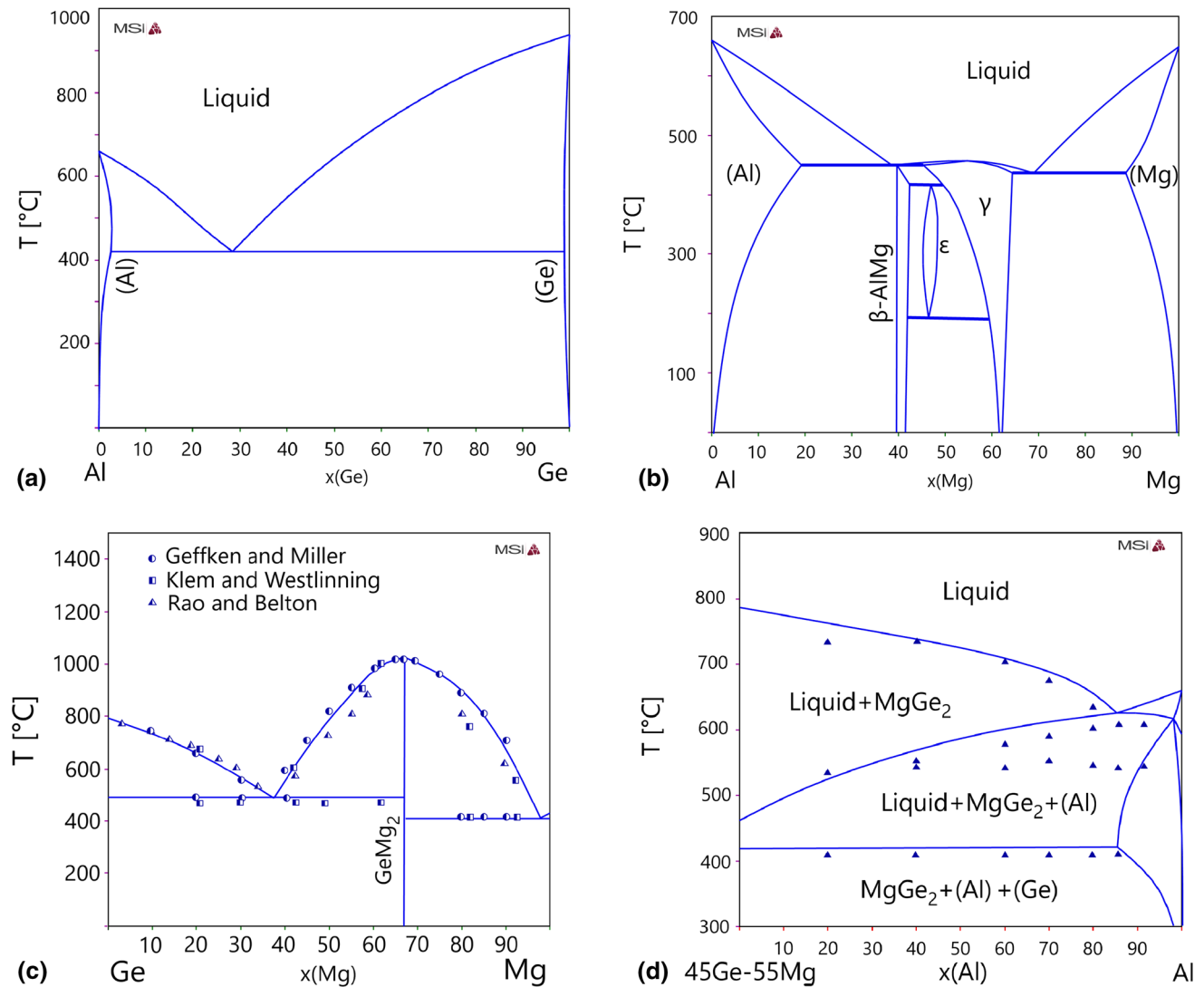


**Fig. 1** Published phase diagrams of relevant systems (a) Al-Ge,<sup>[7]</sup> (b) Al-Mg,<sup>[10]</sup> (c) Ge-Mg,<sup>[12]</sup> (d) Al-Ge-Mg<sup>[8]</sup>

phase diagram of Al–Mg subsystem according to Ren et al.<sup>[10]</sup> is shown on Fig. 1(b).

#### 4 Ge–Mg Binary System

Klemm and Westling<sup>[12]</sup> first established a Ge–Mg binary phase diagram using thermal analysis and microscopic observation. They found that the Ge–Mg binary system contains a single  $\text{GeMg}_2$  intermetallic phase, supposedly with a stoichiometric composition that melts congruently, two eutectic reactions, and a negligible mutual solubility between pure Mg and Ge. These basic features of the phase diagram were subsequently confirmed in Ref 13, 14. Geffken and Miller<sup>[13]</sup> determined the liquidus temperatures for alloys of 10 to 90 at.% Ge by thermal analysis methods. The liquidus line was later experimentally determined

by Rao and Belton<sup>[14]</sup> from discontinuity measurements of EMF vs. temperature curve for alloys in the concentration range 10–95 at.% Ge. The liquidus transition temperatures are approximately 50 °C lower than the values proposed by Geffken and Miller<sup>[13]</sup> and 20 °C lower than the values from Klemm and Westling<sup>[12]</sup> in some regions. A recent thermodynamic review was published by Yan et al.<sup>[15]</sup>. This work is based on the experimental data of Klemm and Westling<sup>[12]</sup> and supported by an ab-initio calculation. They suggested the congruent temperature of the binary  $\text{GeMg}_2$  phase to be 1117 °C. Two eutectic points occur in the phase diagram (see Fig. 1c), the eutectic point in the magnesium-rich part existing at 97.8 at.% Mg and 631 °C, the second eutectic point is located at 37.1 at.% Mg and 699 °C. The solubility in the  $\text{GeMg}_2$  phase was not evaluated in any experimental work for long-term annealed samples. Figure 1(c) shows experimental binary phase

diagram of Ge-Mg subsystem with superimposed experimental data<sup>[12–14]</sup>

## 5 1,4, Al–Ge–Mg Ternary System

The Al-Ge-Mg system has been studied in the past for its potential applications in the aerospace and automotive industries due to its similarity to the Al–Mg–Si system, which is already widely used in this field.<sup>[4,16–18]</sup> B Jorge et al.<sup>[19]</sup> experimentally studied the interface structure of precipitates in Al-0.59 at.% Mg-0.71 at.% Ge alloy. Kawai et al.<sup>[20]</sup> investigated the age hardening of Al-rich samples at 200 °C. Karim et al.<sup>[21]</sup> published an ab-initio study of the optoelectric and thermodynamic properties of the ternary phase  $\tau$ .

The phase equilibria in the Al-Ge-Mg system were experimentally described by Badaeva<sup>[2]</sup> using methods of thermal analysis. Various vertical sections of the phase diagram were investigated. No ternary phase was mentioned in the paper.<sup>[2]</sup> The aluminum-rich part of the phase diagram (up to 10 at.% Al) was also experimentally studied by Legka et al.<sup>[3]</sup> Theoretical modeling of the CALPHAD-based system was performed by Islam<sup>[8]</sup> based on available experimental data. Some experimental points indicating phase transition temperatures were not described and explained in the published assessment. A vertical section of 45 at.% Mg-55 at.% Ge-Al is shown in Fig. 1(d). A set of DTA signals at approx. 550 °C without relevant explanation was found in the Al-rich part. No ternary phase is included in the phase diagram modeling. Recently, Pukas<sup>[4]</sup> published information on a newly prepared ternary intermetallic phase  $\tau$  (Al<sub>2</sub>Ge<sub>2</sub>Mg) with the structure Al<sub>2</sub>Si<sub>2</sub>Ca. The compound was characterized in terms of crystalline structure, thermodynamic and phase properties were not studied. A phase diagram containing the ternary phase has not yet been published. Figure 1(d) shows a vertical Sect. 45 at.% Mg-55 at.% Ge-Al of the Al-Ge-Mg system with the calculated data by Islam<sup>[8]</sup> and superimposed experimental data of Badaeva.<sup>[2]</sup>

## 6 Experimental

The nominal composition of the samples was chosen primarily with the aim to study phase equilibria containing the ternary phase  $\tau$ . The isothermal sections of the ternary phase diagram in the temperature range of 250–450 °C were studied in this work. The long-term annealed samples were characterized using SEM–EDX and XRD.

### 6.1 Sample Preparation

Experimental samples were prepared from high purity metals (5N for Al, Mg and 6N for Ge). The samples were arc-melted on a water-cooled copper plate under a low-pressure 6N Ar atmosphere using pure titanium or magnesium as the getter. The alloys were remelted three times to achieve better sample homogeneity. The alloyed samples were sealed in quartz glass ampoules under vacuum. Vacuumed ampoules with samples were annealed for a long time in a standard muffle furnace. The samples were quenched to cold water from long-term annealing temperatures. Annealing times and temperatures were chosen in order to obtain conditions close to thermodynamic equilibrium.

### 6.2 Experimental Phase Diagram Investigation

The samples were prepared in the metallographic laboratory after long-term annealing. Grinding and polishing were performed under pure ethanol without water to prevent oxidation of the Mg-rich grains. Especially the GeMg<sub>2</sub> grains are very sensitive to oxidation. The overall and coexisting phase compositions were studied by SEM–EDX microanalysis using a JEOL JSM-6460 scanning electron microscope with an EDX Link analyzer from Oxford Instruments (Table 1).

Area analysis was used to determine the overall elemental composition from the representative surface of the sample. For the composition of the coexisting phases, point analysis was used. The grains of various phases were

**Table 1** Stable phases in Al–Ge–Mg ternary system

Phase name [This work]	Other names	Pearson symbol	Structure prototype	T. range, °C	Comments, references
$\alpha$ -Al	FCC_A1	<i>cF4</i>	Cu	< 660	[22]
$\alpha$ -Ge	Diamond_A4	<i>cF8</i>	C	< 938	[22]
$\alpha$ -Mg	HCP_A3	<i>cI2</i>	W	< 650	[22]
$\beta$ -AlMg	Al <sub>3</sub> Mg <sub>2</sub>	<i>cF1832</i>	Al <sub>3</sub> Mg <sub>2</sub>	< 452	[11]
$\gamma$ -AlMg	Al <sub>12</sub> Mg <sub>17</sub>	<i>cI58</i>	$\alpha$ -Mn	< 458	[11]
$\varepsilon$ -AlMg	Al <sub>30</sub> Mg <sub>23</sub>	<i>hR53</i>	Co <sub>5</sub> Cr <sub>2</sub> Mo <sub>3</sub>	185–410	[11]
GeMg <sub>2</sub>	GeMg <sub>2</sub>	<i>cF12</i>	CaF <sub>2</sub>	< 1118	[15]
$\tau$	Al <sub>2</sub> Ge <sub>2</sub> Mg, Al <sub>7</sub> Ge <sub>7</sub> Mg <sub>5</sub>	<i>hP5</i>	CaAl <sub>2</sub> Si <sub>2</sub>	≤ 450	[4, this work]

**Table 2** Cell parameters of ternary phase  $\tau$  with  $\text{CaAl}_2\text{Si}_2$  structure type

Space group	a, Å	c, Å	c/a	V, Å <sup>3</sup>	References
P-3m1	4.11693(5)	6.7873(1)	1.6486	99.627(3)	[4]
P-3m1	4.111987	6.796723	1.6497	99.52532	This work

sufficiently large and with a well-distinguishable contrast in the microscope, so a reliable analysis of the individual phases was possible. The crystallographic structure of the coexisting phases was confirmed by x-ray powder diffraction (XRPD) on an EMPYREAN diffractometer using  $\text{CoK}_\alpha$  radiation Table 2 shows a comparison of the parameters of the ternary phase  $\tau$  cells measured in the scope of this work and the results of Pukas<sup>[4]</sup> analyzed by XRD. Compared to the work of Pukas, the “a” parameter is lower, but the “c” parameter is higher in our sample. The cell volume was lower for the ternary phase found in our work, which supports the idea that smaller magnesium atoms replace the germanium and aluminum atoms with respect to the ideal occupancy in the  $\text{Al}_2\text{Ge}_2\text{Mg}$  stoichiometry.

Representative samples analyzed are listed in Table 3. Column 1 shows the annealing temperature and sample number. The annealing time is given in column 2. The overall composition of the long-term annealed samples is given in column 3. In column 4, the coexisting phases found in a state close to thermodynamic equilibrium are given. The compositions of the equilibrium phases existing in the samples measured by SEM–EDX are shown in column 5.

## 7 Results and Discussion

Using the experimental results of the composition of coexisting phases analyzed by SEM–EDX and listed in Table 3, experimental isotherm sections of the Al–Ge–Mg phase diagram at temperatures of 250 °C, 300 °C, 400 °C and 450 °C were constructed. The overall composition of the studied samples is represented by several symbols in the proposed phase diagrams. The square represents the total composition of samples containing two phases in equilibrium. Just few two-phase samples were found among the samples and the respective composition of each phases and the corresponding connecting tie-lines is shown by dotted line. Triangles represent the total composition of samples containing three phases in equilibrium. Phase compositions are defined by the position of the corners of the connecting triangle and indicated by empty circles. The position of the phase boundaries and the shape of the phase fields not defined by our own samples are drawn as dashed lines and are based on information from the binary subsystems and on the phase rules.

### 7.1 Isothermal Sections

The obtained isothermal sections of the Al–Ge–Mg phase diagram at temperatures of 250, 300, 400 and 450 °C are shown in Fig. 2. The isothermal sections look very similar in this range. The numbers given refer to the sample number annealed at the given temperature. The characteristic morphology of concrete phase structures describing the various phase fields are shown in micrographs in Fig. 3. All the micrographs are visualized in BSE mode. Figure 3(a) is a sample No 250\_2 annealed at 250 °C consisting of the three phases  $\alpha$ -Al,  $\text{GeMg}_2$  and  $\tau$ , where the ternary  $\tau$  phase is a matrix. Figure 3(b) shows a sample No 250\_3 annealed at 250 °C consisting of the three phases  $\alpha$ -Al,  $\alpha$ -Ge and  $\tau$ , where the  $\alpha$ -Ge is a matrix. Figure 3(c) shows microstructure of the sample No 300\_4 annealed at 300 °C in consisting of the phases  $\alpha$ -Al,  $\alpha$ -Ge and  $\tau$ . Figure 3(d) represents a microstructure of the sample No 300\_5 annealed at 300 °C in BSE mode consisting of the phases  $\alpha$ -Al,  $\text{GeMg}_2$  and  $\beta$ -AlMg where the  $\beta$ -AlMg is a matrix. Figure 3(e) is the sample No 400\_4 annealed at 400 °C consisting of the phases  $\alpha$ -Al,  $\text{GeMg}_2$  and  $\beta$ -AlMg, where the  $\beta$ -AlMg is a matrix. Figure 3(f) is a microstructure of the sample No 400\_5 annealed at 400 °C in BSE mode consisting of the phases  $\alpha$ -Al,  $\alpha$ -Ge and  $\tau$ . Figure 3(g) shows a Microstructure of the sample No 450\_5 annealed at 450 °C in BSE mode consisting of the phases  $\alpha$ -Al,  $\text{GeMg}_2$  and  $\tau$ , where the ternary  $\tau$  phase is a matrix.

Aluminum ( $\alpha$ -Al) and magnesium ( $\alpha$ -Mg) show a very limited solubility of germanium in their structure. On the other hand, germanium shows a relatively high ternary solubility of magnesium compared to the published Ge–Mg binary phase diagram (see Fig. 1c). In the theoretically evaluated Ge–Mg binary phase diagram published by Yan et al. no solubility of magnesium in germanium was considered.<sup>[15]</sup> As mentioned in the Sect. 1.3, no previous experimental work on Ge–Mg system has studied the mutual solubility of both elements,<sup>[12,13]</sup> and<sup>[14]</sup> used mainly thermal analysis and EMF measurements. We experimentally found the solubility of up to 6% Mg in Ge in the Al–Ge–Mg ternary system. The measured solubility of Mg in Ge in the ternary system is generally consistent for all isothermal section at specific temperatures and indicates a slow decrease in solubility with increasing temperature.

**Table 3** Chemical composition of the long-term annealed representative sample

T, °C No	Annealed time, h	Overall composition, at. %			Coexist. phases	Phase composition, at. %		
		Al	Ge	Mg		Al	Ge	Mg
250_1	5052	23.5	43.2	33.3	$\alpha$ -Ge	4.0	93.8	2.2
					GeMg <sub>2</sub>	0.7	28.1	71.2
					$\tau$	34.5	36.5	29.0
250_2	5052	67.1	17.7	15.2	$\alpha$ -Al	98.7	1.2	0.1
					GeMg <sub>2</sub>	1.2	27.8	71.0
					$\tau$	36.8	34.4	28.8
250_3	5052	63.9	32.9	3.2	$\alpha$ -Al	98.4	1.6	0.0
					$\alpha$ -Ge	2.4	92.1	5.5
					$\tau$	38.2	36.2	25.6
250_4	5052	60.4	3.5	36.1	GeMg <sub>2</sub>	*	*	*
					$\alpha$ -Al	92.0	7.5	0.5
					$\beta$ -AlMg	61.1	0.5	38.4
250_5	5052	19.0	5.6	75.4	Mg	3.9	1.0	95.1
					$\gamma$ -AlMg	34.0	1.1	64.9
					GeMg <sub>2</sub>	0.8	25.8	73.4
300_1	2304	22.0	51.9	26.1	$\alpha$ -Ge	3.7	91.7	4.6
					GeMg <sub>2</sub>	0.4	31.3	68.3
					$\tau$	34.1	36.5	29.4
300_2	2304	67.4	17.5	15.1	$\alpha$ -Al	97.5	2.2	0.3
					GeMg <sub>2</sub>	2.3	27.5	70.2
					$\tau$	39.7	33.6	26.7
300_3	2304	65.9	31.8	2.3	$\alpha$ -Al	98.2	1.8	0.0
					$\alpha$ -Ge	3.0	90.6	6.4
					$\tau$	37.2	36.9	25.9
300_4	3427	54.8	32.4	12.8	$\alpha$ -Al	98.4	1.6	0.0
					$\alpha$ -Ge	3.2	93.9	2.9
					$\tau$	34.6	37.1	28.3
300_5	3427	65.6	7.0	27.4	$\alpha$ -Al	88.5	10.6	0.1
					GeMg <sub>2</sub>	2.9	25.8	71.3
					$\beta$ -AlMg	66.2	0.9	32.8
300_6	3427	58.9	3.4	37.7	$\alpha$ -Al	84.0	0.5	15.5
					GeMg <sub>2</sub>	2.2	25.8	72.0
					$\beta$ -AlMg	60.8	0.4	38.8
300_7	3427	15.7	7.6	76.7	$\alpha$ -Mg	7.0	1.1	91.9
					GeMg <sub>2</sub>	1.1	26.0	72.9
					$\gamma$ -AlMg	32.5	0.9	66.6
400_1	1976	85.6	14.3	0.1	$\alpha$ -Al	97.2	2.8	0.0
					$\alpha$ -Ge	2.0	92.2	5.8
					$\tau$	37.3	38.7	24.0
400_2	1976	67.9	30.3	1.8	$\alpha$ -Al	97.1	2.9	0.0
					$\alpha$ -Ge	2.7	91.6	5.7
					$\tau$	35.9	41.2	22.9
400_3	2567	67.0	23.1	9.9	$\alpha$ -Al	97.1	2.9	0.0
					$\alpha$ -Ge	1.5	95.0	3.5
					$\tau$	36.6	37.4	26.0
400_4	2567	54.9	10.1	35.0	$\alpha$ -Al	82.4	0.8	16.8
					GeMg <sub>2</sub>	1.5	27.7	70.9

**Table 3** continued

T, °C No	Annealed time, h	Overall composition, at. %			Coexist. phases	Phase composition, at. %		
		Al	Ge	Mg		Al	Ge	Mg
400_5	2567	58.3	29.4	12.3	$\beta$ -AlMg	63.1	1.1	35.8
					$\alpha$ -Al	96.8	3.1	0.1
					$\alpha$ -Ge	3.2	91.7	5.1
400_6	2567	71.2	11.8	17.0	$\tau$	37.0	36.7	26.3
					$\tau$	37.3	34.5	28.2
					$\alpha$ -Al	98.9	1.1	0.0
400_7	2567	22.9	46.6	30.5	$\text{GeMg}_2$	*	*	*
					$\tau$	35.4	36.2	28.4
					$\alpha$ -Ge	5.5	86.2	8.3
400_8	2567	42.3	34.0	23.7	$\text{GeMg}_2$	0.6	29.1	70.3
					$\tau$	35.5	36.5	28.0
					$\alpha$ -Al	98.1	1.8	0.1
450_1	1319	23.5	46.0	30.5	$\alpha$ -Ge	2.2	92.1	5.7
					$\text{GeMg}_2$	0.1	29.9	70.0
					$\tau$	35.5	36.0	28.5
450_2	1319	71.9	15.6	12.5	$\alpha$ -Al	98.8	1.2	0.0
					$\text{GeMg}_2$	0.5	28.7	70.8
					$\tau$	38.1	32.9	29.0
450_3	1319	50.4	44.9	4.7	$\alpha$ -Ge	1.8	93.3	5.0
					$\tau$	36.3	38.1	25.7
					Liquid	65.3	32.1	2.6
450_4	3288	59.2	29.1	11.7	$\alpha$ -Al	96.4	3.5	0.1
					$\tau$	36.8	36.8	26.4
					Liquid	74.1	24.7	1.2
450_5	3288	77.3	8.5	14.2	$\alpha$ -Al	98.0	1.1	0.9
					$\text{GeMg}_2$	1.9	36.8	71.3
					$\tau$	35.8	34.9	29.3
450_6	3288	38.9	31.4	29.7	$\tau$	35.7	36.2	28.1
					$\alpha$ -Al	96.0	2.9	1.1
					$\text{GeMg}_2$	1.2	28.5	70.3
450_7	3288	42.3	34.0	23.7	$\tau$	35.5	36.5	28.0
					$\alpha$ -Al	95.8	3.4	0.8
					$\text{GeMg}_2$	1.1	23.8	75.1
450_8	3288	78.8	7.3	13.9	$\alpha$ -Al	99.1	0.8	0.1

\*Not measurable

The solubility of Al in Ge solid solution in the Al-Ge-Mg ternary system is slightly higher than that in the Al-Ge binary system. Again, the consistency of the measured values in this work is very good. Here the increase in solubility could be attributed to the influence of the third element in the studied system. Nevertheless, a new detailed study of at least the Ge-Mg binary system is necessary.

The  $\beta$ -AlMg and  $\gamma$ -AlMg binary phases show very limited solubility of germanium. The binary phase of  $\epsilon$ -AlMg was not found in our samples, since our main goal was to find phase equilibria with the ternary phase  $\tau$  and we

chose the nominal compositions of studied samples accordingly. The solubility of Ge in  $\epsilon$ -AlMg was estimated to be very small, consistent with measured solubility in other intermetallic phases in the Al-Mg system and the relevant phase fields were drawn by dashed lines.

We found only very limited solubility of germanium in magnesium solid solution in the relevant samples annealed at 250 and 300 °C, as shown in Fig. 2(a) and (b). Considering the limited information about the solubility in the Ge and Mg solid solutions, this result is in good agreement with the Ge-Mg binary phase diagram (Fig. 1c).



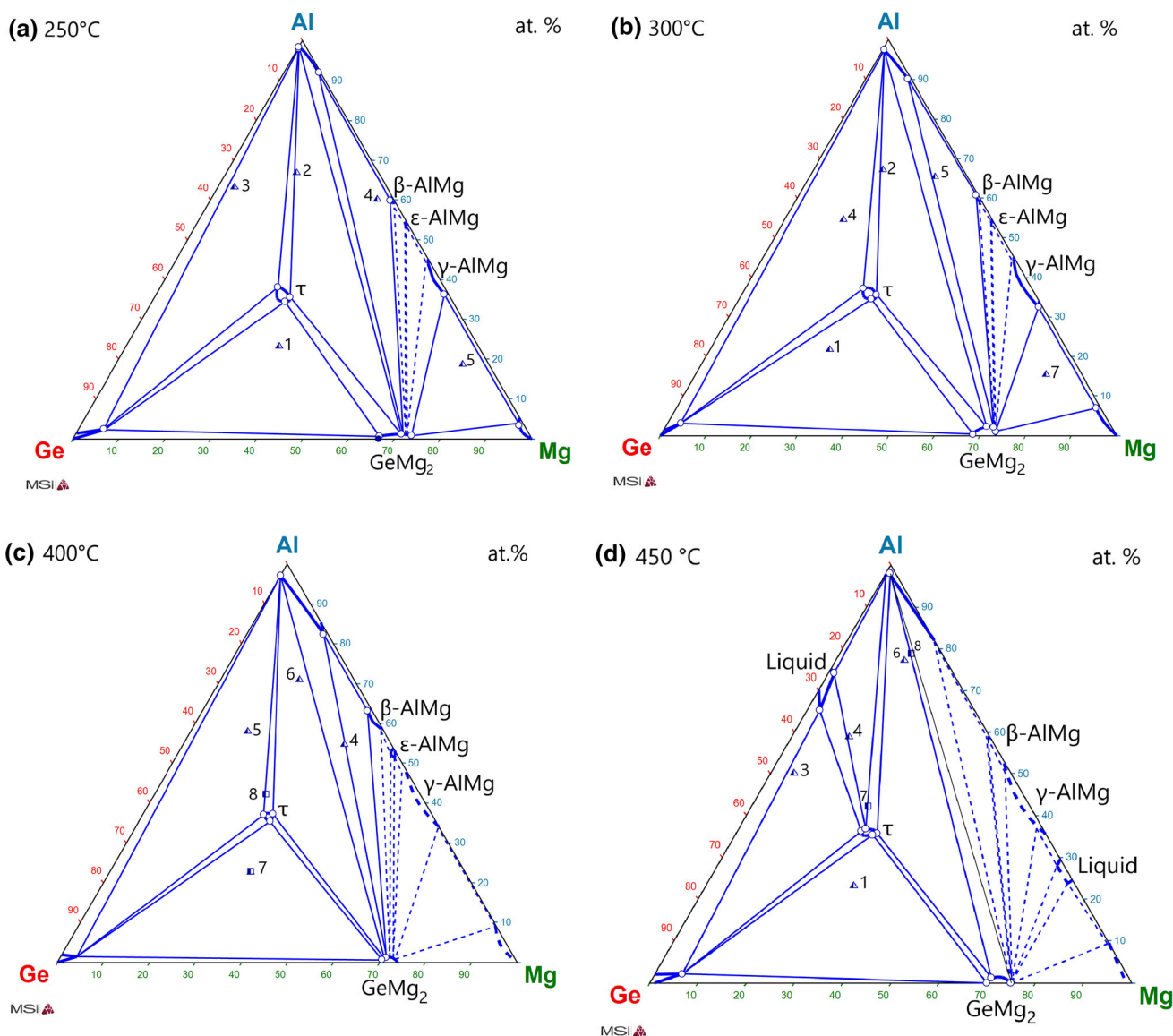


**Fig. 2** Isothermal section of experimental Al-Ge-Mg ternary phase diagram at (a) 250 °C (b) 300 °C (c) 400 °C and (d) 450 °C

The  $\text{GeMg}_2$  phase shows an extended range of composition between 66 and 73 at.% Mg at temperatures of 250 to 300 °C (Fig. 2a and b). The XRD pattern of sample No. 300\_7 (15.7 at.% Al-7.6 at.% Ge-Mg) containing a reasonable amount of  $\text{GeMg}_2$  phase is shown in Fig. 4(a), where the binary phases  $\text{GeMg}_2$ ,  $\gamma\text{-AlMg}$  and magnesium coexist. At higher temperatures, the  $\text{GeMg}_2$  phase shows only limited solubility around 72 at.% Ge (Fig. 2c and d). Again this finding contradicts the previously assessed Ge-Mg phase diagram published by Yan et al.,<sup>[15]</sup> where the  $\text{GeMg}_2$  phase is linear with a composition of 66.6 at.% Mg. On the other hand, the modeling performed by<sup>[15]</sup> was based on limited experimental thermal analysis and EMF data only (<sup>[12,13]</sup> and<sup>[14]</sup>), the solubility of the

intermetallic phase has not been studied experimentally in any previous work to the best of our knowledge.

The ternary phase  $\tau$  was found to be stable at all studied temperatures up to 450 °C and slightly nonstoichiometric with similar solubility of a few percent for all elements. In his study, Pukas<sup>[4]</sup> described crystallographic structure of this phase as a stoichiometric one with an  $hP5$  structure of the  $\text{Al}_2\text{Si}_2\text{Ca}$  type. This structure for the experimentally found ternary phase  $\tau$  in this study was confirmed by the XRD analysis (see Fig. 4b), but its experimentally measured composition is shifted and the center of the single-phase region is located at approx. 36 at.% Al-Ge-28 at.% Mg. This composition is consistent for all temperatures and all relevant samples containing three-phase equilibria with the  $\tau$  phase (see Table 3).

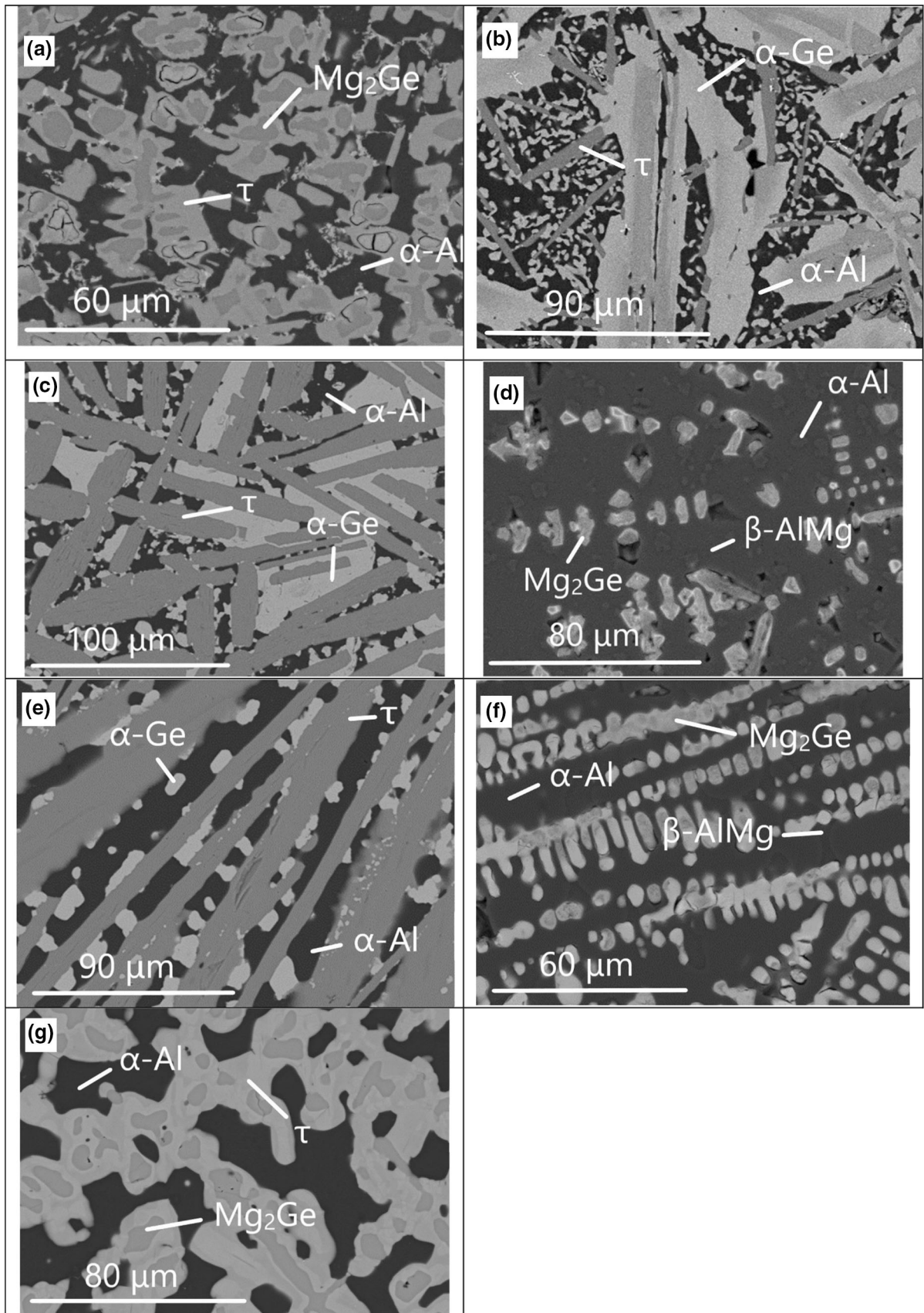




**Fig. 3** Microstructures in BSE mode of long-term annealed samples (a) 250\_2, (b) 250\_3, (c) 300\_4, (d) 300\_5, (e) 400\_4, (f) 400\_5 and (g) 450\_5

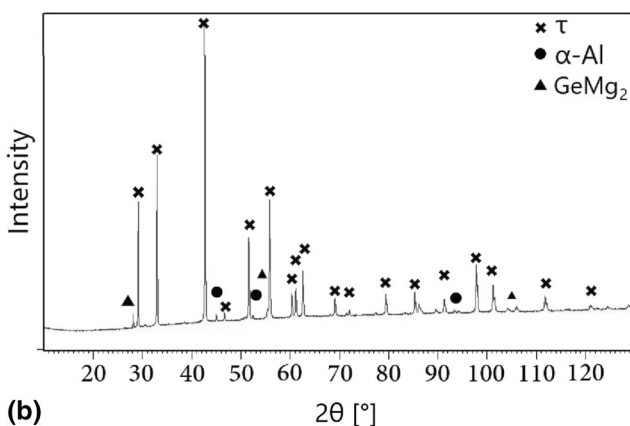
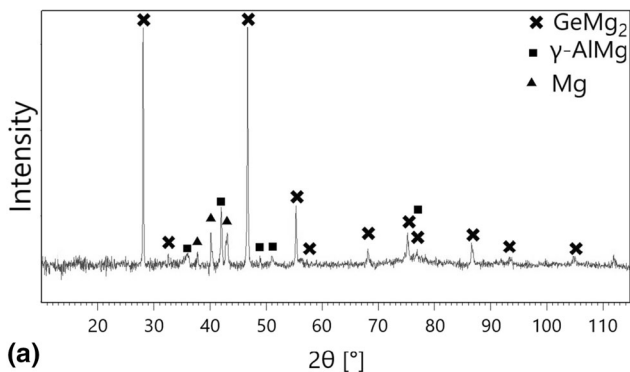


**Fig. 4** XRD patterns of samples (a) 300\_7 where the binary phases  $\text{GeMg}_2$ ,  $\gamma\text{-AlMg}$  and magnesium coexist and (b) 400\_8, where the 92.6% of ternary phase  $\tau$ , 4.3  $\text{GeMg}_2$  phase and the 3.1% of pure aluminum coexist

## 8 Conclusion

Although there is literature regarding the Al-Ge-Mg phase diagram [2, 2019Leg], complex phase equilibria with recently described ternary phase<sup>[4]</sup> have not been yet studied. This study was designed to contribute to a better understanding of the stability of the this ternary phase  $\tau$ . Experimental studies were carried out at temperatures of 250 °C, 300 °C, 400 °C and 450 °C. Isothermal sections of the Al-Ge-Mg ternary phase diagram were obtained by a combination of standard methods: the overall and phase compositions of the samples were measured by SEM–EDX and the crystal structures were identified by XRD. Following key results were obtained in the scope of this work:

- Significant nonstoichiometricity of the binary intermetallic phase  $\text{GeMg}_2$  was observed at 250 °C [ $x(\text{Mg}) = 0.666\text{--}0.735$ ] and 300 °C [ $x(\text{Mg}) =$

$0.68\text{--}0.734$ ]. Its position at 400 and 450 °C is close to  $x(\text{Mg}) = 0.73$ .

- The ternary phase  $\tau$  was found to be stable at all temperatures studied.
- The composition of the  $\tau$  phase was found to be close to 36 at.% Al-Ge-28 at.% Mg, which does not correspond to the published composition of 40 at.% Al-40 at.% Ge-20 at.% Mg proposed by Pukas.<sup>[4]</sup>
- Significant differences were found for the solubility of Mg in the Ge solid solution and extent of solubility of the  $\text{GeMg}_2$  phase with respect to the existing Mg-Ge phase diagram of Ref 12–14 With respect to the consistency of results obtained in the scope of this work, the new study of the binary system is planned.

**Acknowledgments** This study was funded by Czech Science Foundation of Czech Republic (Grant No. GA 22-22187S).

**Funding** Open access publishing supported by the National Technical Library in Prague.

**Open Access** This article is licensed under a Creative Commons Attribution 4.0 International License, which permits use, sharing, adaptation, distribution and reproduction in any medium or format, as long as you give appropriate credit to the original author(s) and the source, provide a link to the Creative Commons licence, and indicate if changes were made. The images or other third party material in this article are included in the article's Creative Commons licence, unless indicated otherwise in a credit line to the material. If material is not included in the article's Creative Commons licence and your intended use is not permitted by statutory regulation or exceeds the permitted use, you will need to obtain permission directly from the copyright holder. To view a copy of this licence, visit <http://creativecommons.org/licenses/by/4.0/>.

## References

1. F. Ning, Z. Chunming, W. Zunije, W. Hongwei, Z. Xuejian, and C. Tao, Effect of Ge and Mg Additions on the Aging Response Behavior and Mechanical Properties of Al–Si–Cu Alloy, *Mater. Sci. Eng. A.*, 2021, **811**, 141024.
2. T. Badaeva, and R. Kuznetsova, Liquidus Surface and Aluminum Solid Solutions in the Al–Mg–Ge System, *Metalloved. Term. Obrab. Met.*, 1958, **3**, p 216–230.
3. T.M. Legka, T.M. Mika, Y.V. Milman, N.P. Korzhova, I.V. Voskoboinik, and N.M. Mordovets, Constitution of the Al Corner in the Ternary Al–Ge–Mg Phase Diagram, *Powder Metall. Met. Ceram.*, 2019, **57**(11–12), p 716–722.
4. S. Pukas, L. Pylypchak, O. Matselko, P. Demchenko, and R. Gladyshevskii,  $\text{MgAl}_2\text{Ge}_2$  – A New Representative of the Structure Type  $\text{CaAl}_2\text{Si}_2$ , *Chem. Met. Alloys*, 2012, **5**(1/2), p 59–65.
5. I. Ansara, J.P. Bros, and M. Gambino, Thermodynamic Analysis of the Germanium-Based Ternary Systems (Al–Ga–Ge, Al–Ge–Sn, Ga–Ge–Sn), *CALPHAD: Comput. Coupl. Phase Diagr. Thermochem.*, 1979, **3**(3), p 225–233.
6. H. Eslami, J. de Franceschi, M. Gambino, and J.P. Bros, An Electromotive-Force Study of the Activity of Aluminum in Al–

- Ga, Al-Ge and Al-Ga-Ge Systems, *Z Für Naturforschung A*, 1979, **34**(7), p 810–817.
7. A.J. McAlister, and J.L. Murray, The Al-Ge (Aluminum-Germanium) System, *Bull. Alloy Phase Diagr.*, 1984, **5**(4), p 341–347.
  8. F. Islam, A.K. Thykadavil, and M. Medraj, A Computational Thermodynamic Model of the Mg–Al–Ge System, *J. Alloys Compd.*, 2006, **425**(1), p 129–139.
  9. P. Liang, H.L. Su, P. Donnadiou et al., Experimental Investigation and Thermodynamic Calculation of the Central Part of the Mg – Al Phase Diagram, *Int. J. Mater. Res.*, 1998, **89**(8), p 536–540.
  10. Y.P. Ren, G.W. Qin, S. Li, Y. Guo, X.L. Shu, L.B. Dong, H.H. Liu, and B. Zhang, Re-Determination of  $\gamma/(\gamma+\alpha\text{-Mg})$  Phase Boundary and Experimental Evidence of R Intermetallic Compound Existing at Lower Temperatures in the Mg–Al Binary System, *J. Alloys Compd.*, 2012, **540**, p 210–214.
  11. R. Shi, Z. Zhu, and A.A. Luo, Assessing Phase Equilibria and Atomic Mobility of Intermetallic Compounds in Aluminum-Magnesium Alloy System, *J. Alloys Compd.*, 2020, **825**, 153962.
  12. W. Klemm, and H. Westlinning, Untersuchungen über die Verbindungen des Magnesiums mit den Elementen der IV b-Gruppe, *Z. anorg. allg. Chem.*, 1941, **245**, p 365–380.
  13. R. Geffken, and E. Miller, Phase Diagrams and Thermodynamic Properties of the Mg-Si and Mg-Ge Systems, *Trans. Metall. Soc. AIME*, 1968, **242**, p 2323.
  14. Y.K. Rao, and G.R. Belton, Thermodynamic Properties of Mg–Ge Alloys, *Metall. Trans.*, 1971, **12**, p 2215–2219.
  15. H. Yan, Y. Du, L. Zhou, H. Xu, L. Zhang, and S. Liu, Reassessment of the Mg–Ge Binary system Using CALPHAD Supported by First-Principles Calculation, *Int. J. Mater. Res.*, 2010, **101**(12), p 1489–1496.
  16. K. Matsuda, S. Ikeno, and T. Munekata, HRTEM Study of Precipitates in Al-Mg-Si and Al-Mg-Ge Alloys, *Mater. Sci. Forum*, 2006, **519–521**, p 221–226.
  17. K. Matsuda, T. Munekata, and S. Ikeno, Effect of Mg Content on the Precipitation in Al-Mg-Ge Alloys, *S. Mater. Sci. Forum*, 2007, **561–565**, p 2049–2052.
  18. R. Bjørge, C.D. Marioara, S.J. Andersen, and R. Holmestad, Precipitation in Two Al-Mg-Ge Alloys, *Metall. Mater. Trans. A*, 2010, **41**, p 1907.
  19. R. Bjørge, P.N.H. Nakashima, C.D. Marioara, S.J. Andersen, B.C. Muddle, J. Etheridge, and R. Holmestad, Precipitates in an Al–Mg–Ge Alloy Studied by Aberration-Corrected Scanning Transmission Electron Microscopy, *Acta Mater.*, 2011, **59**, p 6103–6109.
  20. A. Kawai, K. Watanabe, K. Matsuda, and S. Ikeno, The Age-Precipitations Structure of Al–Mg–Ge Alloy Aged At 473K, *Arch. Metall. Mater.*, 2015, **60**(2), p 969–970.
  21. A.M.M.T. Karim, M.A. Helal, M.A. Alam, M.A. Ali, I. Ara, and S.H. Naqib, Optoelectronic, Thermodynamic and Vibrational Properties of Intermetallic  $\text{MgAl}_2\text{Ge}_2$ : A First-Principles Study, *SN Appl. Sci.*, 2021, **3**, p 229.
  22. P. Villars Pearson’s handbook crystallographic data for intermetallic phases, ASM International 1997.

**Publisher’s Note** Springer Nature remains neutral with regard to jurisdictional claims in published maps and institutional affiliations.